Medjem 2019

by Poedji Lh

Submission date: 02-Jan-2022 01:19PM (UTC+0700)
Submission ID: 1736826967
File name: 4a_MEDJCHEM_2019.pdf (517.23K)
Word count: 5845
Character count: 29871

Available free online at www.medjchem.com

Mediterranean Journal of Chemistry

Mediterranean Journal of Chemistry **2019**, 9(2), 85-94

Kinetic and thermodynamic adsorption of nickel (II) onto hydroxyapatite prepared from Snakehead (*Channa striata*) fish bone

Poedji Loekitowati Hariani * Muryati and Muhammad Said

Department of Chemistry, Faculty of Mathematics and Natural Sciences, Sriwijaya University, Ogan Ilir 30662, Indonesia

Abstract: Biomaterial exploration base on solid waste has been an attractive issue, particularly regarding economic and environmental demand. This work aimed to extract hydroxyapatite from snakehead fishbone through precipitation method and used to remove Ni(II). The hydroxyapatite product was characterized by using X-ray Diffraction (XRD), Fourier Transform Infrared spectroscopy (FTIR), Scanning Electron Microscope-Energy Dispersive Spectroscopy (SEM-EDS) and Brunauer Emmett Teller (BET) method. Batch adsorption experiment includes pH solution, contact time and Ni(II) concentration. Pseudo-first order and pseudo-second-order were used to investigate the reaction mechanism and kinetic model, while adsorption equilibrium was evaluated according to Langmuir and Freundlich isotherm. XRD and FTIR spectra confirmed that hydroxyapatite was successfully extracted. The molar ratio (Ca/P) of hydroxyapatite was found at 1.70. The particle size of the hydroxyapatite was 48.77 nm. The pseudo-second-order is appropriate to describe the kinetic model while the adsorption mechanism follows Langmuir isotherm, which has an adsorption capacity of 5.359mg/g. The thermodynamic evaluation suggested the adsorption of Ni(II) is spontaneous in the endothermic process.

Keywords: snakehead fish bone, hydroxyapatite, adsorption, Ni(II)

1. Introduction

Advanced industrial activity creates massive ecosystem damage in the form of a harmful pollutant for both human and environment. One of the related issues that have been reported by many authors is heavy metal removal from liquid waste which pollutes the aquatic environment [1]. Heavy metal ions in low level such as nickel, lead, cadmium, copper etc… are non-biodegradable and hazardous [2]. Furthermore, heavy metal tends to bioaccumulate in the environment, which makes it more risk [3]. Nickel is classified as a heavy metal that used in much industrial application such as metal alloy, paint, printing, electroplating, plastic, battery, electric power and mining which can be released to the environment as Ni(II) [4,5]. Some anions correlated to Ni(II) such as sulfide, nitrate, chloride interact chemically to form salts that dissolved in water. Intake of Ni(II) into the human body caused several health problems, e.g. skin dermatitis, anaemia, indigestion, hepatitis, and lung and kidney damage [3,4,5]. Ni(II) accumulation in the long term creates a high concentration within the body which can lead to lung as well as nose and bone cancer [3,6]. According to the World Health Organization, the maximum of Ni in drinking water is 0.5 mg/L. Therefore, it is essential to reduce Ni(II) in aqueous so as not to pollute the environment.

A heavy metal pollutant can be removed by several methods, i.e. filtration, ion exchange, reduction-oxidation, flocculation, chemical precipitation, membrane, and adsorption. Among these methods, adsorption is acclaimed as the most straightforward, low cost and effective way to remove pollutants [7,8]. The adsorbent can be sourced from various organic and inorganic materials. Attention has been grown on using low-cost natural-based adsorbent. Several authors had been reported using biomaterial in Ni(II) adsorption such as physic seed hull [2], calotropis procera [3], mustard oil cake [5], activated carbon from coir pith [6], bovine bond [9], moringa oleifera bark [10], and pseudomonas oleovorans [11].

Hydroxyapatite is a biomaterial that has structure and composition similar to natural bone [12]. It is highly biocompatible with skin and dental gums so that it can use as bone and dental implant [13]. Hydroxyapatite can also be used as a catalyst, ion exchange, and adsorbent [14,15]. The molecular structure of this material is $Ca_{10}(PO_4)_6(OH)_2$ which resembles an apatite compound. Several authors used hydroxyapatite for pollutant removal due to high affinity, low solubility, high stability, and economical [1,16,17]. Among waste

**Corresponding author: Poedji Loekitowati Hariani*
Email address: puji_lukitowati@mipa.unsri.ac.id
DOI: http://dx.doi.org/10.13171/mjc92190906825plh

Received July 12, 2019
Accepted August 1, 2019
Published September 6, 2019

and pollutants reported being removed by hydroxyapatite were zinc [1], reactive blue [8], copper [16], strontium [18], oxytetracycline [19], and lead [20]. The mechanism of heavy metal ion adsorption by hydroxyapatite involve Ca cation exchange within its structure [16,21]. In addition to cation adsorption, hydroxyapatite was also reported for anion adsorption such as fluoride [22].

There are a variety of sources can be used to synthesize hydroxyapatite. Calcium contains biomaterial, as well as biowaste, can be used for this purpose such as swordfish and tuna [12], eggshell [15], Roho labio fish bone [23], oyster shell[24] and pensi shell [25]. Using biowaste for hydroxyapatite synthesis provide some advantages i.e. low cost, available in abundant amount and also environmentally friendly. Fishbone shows great potential for the production of hydroxyapatite because millions of tons of fish were captured and consumed worldwide annually [26]. Consumption of fish provides solid wastes estimate of 30-40% ie bone, scale, skin [21]. Such a vast number of wastes undoubtedly caused serious environment problem as well as health disorders. High calcium content within fish bone made this material a good precursor for hydroxyapatite synthesis.

Hydroxyapatite in this work was synthesized from snakehead (*Channa striata*) fish bone. Snakehead is a freshwater fish, the name of residents as *Gabus* fish. This fish has been cultivated for a long time ago. The method of hydroxyapatite preparation such as heat treatment [23], co-precipitation [24,27], sol-gel [28], combustion [29] and ultrasonic [30]. The choice of preparation method will affect hydroxyapatite crystallinity, the molar ratio of Ca/P, and particle size [31]. Precipitation method is also classified as wet chemical precipitation has been widely used in hydroxyapatite synthesis because of its simplicity and high yield of product [32]. Generally, hydroxyapatite was synthesized in the form of the nanoparticle. The material in nanosize has a surface area, and high reactivity is more significant compared to bulk material [33]. Hydroxyapatite obtained in this work was characterized using XRD, FTIR, SEM-EDS and BET method. This material was tested in Ni(II) adsorption from aqueous solution.

2. Experimental

2.1. Material

Snakehead fish was acquired from the domestic market located in Palembang, South Sumatera, Indonesia. Chemicals were purchased from Merck (Germany) in analytical grade i.e. HCl, $(NH_4)_2HPO_4$, NH_4OH, $NiCl_2.6H_2O$, NaOH. The solvent in the majority of procedures used double distilled water.

2.2. Hydroxyapatite synthesis [34]

Fishbone was cleaned of dirt and washed using distilled water and boiled for 90 minutes to remove the flesh. The fish bones were cut to obtain 5 mm in size followed by reflux method using HCl 4% for 30 minutes. After that, the fishbone was neutralized using distilled water. The bone heating in an oven at 100°C for 2 hours followed by calcination in a muffle furnace for 4 hours at 800 °C with a heating rate was set of 10°C/min. This process converts $CaCO_3$ to CaO. CaO product was crushed into nanosized by using high energy ball milling (Shaker mill PPF-UG) for 5 hours to obtain a powder. 2.8 g of powder CaO was added of 250 mL distilled water and boiled for one hour. 150 mL $(NH_4)_2HPO_4$ (0.2 M) was added into the solution in an inert atmosphere by flowing N_2. The mixture was heated at 100°C while NH_4OH 1 M was added dropwise until pH reaches 11. Hydroxyapatite was collected by filtration and drying in the oven at 105°C for 2 hours.

2.3. Characterization of hydroxyapatite

Functional groups in hydroxyapatite were evaluated by using Fourier Transform Infrared (FTIR Thermo Scientific Nicolet iS10) and applying KBr pellet scanned at wavenumber range 4000-500 nm^{-1}. The morphology was observed using Scanning Electron Microscope (SEM-EDS VEGA 3 TESCAN) equipped with EDS (Energy Dispersive X-ray Spectroscopy) to determine hydroxyapatite element content. The surface area of hydroxyapatite was measured by the BET method using N_2 adsorption-desorption (Nova 4200e).

The phase composition of the hydroxyapatite was characterized by using X-ray diffraction (XRD Rigaku Miniflex 600) using Cu Kα radiation (λ = 0.15406 nm) at 2θ range 10-80°. The average particle size (d) was determined by using the Debye-Scherrer equation [12,34]:

$$d = \frac{k\,\lambda}{\beta\,\cos(\theta)} \quad (1)$$

Where k is a constant associated with the crystal shape (0.9), β is a full-width peak at half maximum intensity (rad), λ is X-Ray radiation wavelength (1.5418 Å). Data used to calculate particle size was based on line broadening at reflection plane (211), assuming that it provides excellent resolution and no interference occurred.

2.4. Adsorption of Ni(II)

The adsorption of Ni(II) was conducted in the batch method. pH_{PZC} obtained by 50 mg of adsorbent was put into 50 mL of 0.5 M KCl, pH of the solution made from 3 to 10 with addition HCl and NaOH 0.01 M. After 24 hours, obtained the pH of the solution. The optimum condition for adsorption was evaluated by varying the solution pH, contact time and initial concentration of Ni(II). Determination of optimum pH was conducted by 0.1 g of hydroxyapatite was dispersed in 50 mL Ni(II) solution with a concentration of 30 mg/L. The mixture was stirred at 150 rpm and a temperature of 25°C for 100 minutes. Solution pH was varied in range 3-10 by adding HCl and NaOH. After adsorption, the solution determined of Ni (II) concentration which is not absorbed by

Atomic Absorption Spectroscopy (AA-7000 Shimadzu). Contact time for adsorption was evaluated by using a similar procedure with time as variable i.e. 10 to 120 minutes. The initial concentration of Ni(II) was set at a different amount ranged from 10 to 30 mg/L. The experiment was carried out triplicate.

3. Results and Discussion

3.1. Characterization of hydroxyapatite

The crystal structure of fishbones and hydroxyapatite was evaluated using XRD, as shown in Figure 1. The amorphous structure of fishbone can be seen as a wide peak on the diffractogram obtained. Also, hydroxyapatite appears at a sharp peak higher than fish bone. According to JCPDS 09-0432, hydroxyapatite has hexagonal crystal showing peaks at 2θ = 25.879; 31.773; 32.196; 32.902; 46.711; 49.468; 50.493 and 53.143° which correspond with reflection plane 002, 211, 112, 300, 202, 310, 222, 213, 321 and 004 [7]. Diffractogram of hydroxyapatite in this work shows peaks at 2θ = 25.98; 31.92; 32.98; 33.03; 46.80; 49.58; 50.56 and 53.26°. The particle size of hydroxyapatite calculated by using Debye-Scherrer is ± 48.77 nm. Based on this result, the material obtained is nanoparticle (<100 nm) or nano-hydroxyapatite [35].

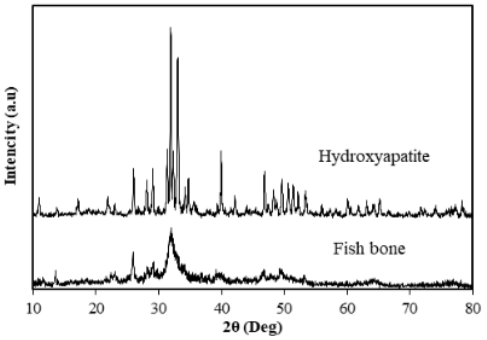

Figure 1. X-ray diffractogram of hydroxyapatite

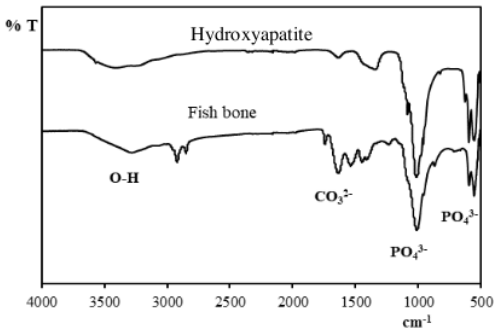

Figure 2. FTIR spectra of hydroxyapatite

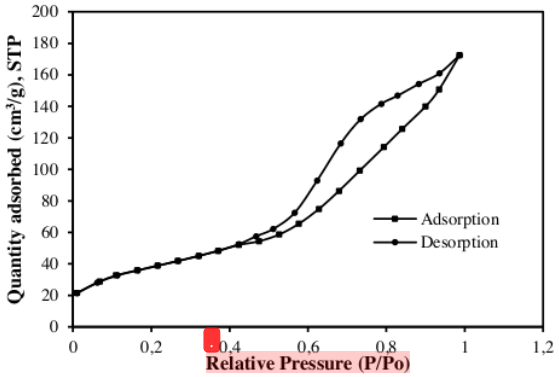

Figure 3. N_2 adsorption-desorption isotherm of hydroxyapatite

Hydroxyapatite prepared from snakehead fish bone has FTIR spectra (Figure 2) similar to hydroxyapatite synthesized from bovine bone [9] and *Lates calcarifer* fish bone [36]. The P-O group can be identified at the wavenumber of 500-1100 cm^{-1}. The FTIR spectra of hydroxyapatite showed peaks at wavenumber 542 and 594 cm^{-1} that resemble vibration mode of the P-O group while the vibration stretch for this bond appears at 993 cm^{-1}. The sharp peak at 1010 cm^{-1} also assigned for P-O bond from PO_4^{3-}. Fishbone powder reveals similar peaks at a lower intensity. Therefore, the powder contains a phosphate group within its structure. High and sharp peaks belonging to fish bone powder appeared at wavenumber 1400 and 1420 cm^{-1} which indicate the existence of C-O stretching from carbonate group (CO_3^{2-}). Another possibility for this peak comes from CO_2 adsorbed on hydroxyapatite surface [37,38]. Stretching vibration from O-H group at with wavenumber 3210 and 3530 cm^{-1} correspond with the presence of H_2O. The main difference of FTIR spectra between fish bone powder and hydroxyapatite lies on peaks at 2840 and 2910 cm^{-1} also supported by 1600 cm^{-1} which represents N-H absorption band of protein contained in the fish bone powder.

The surface area of hydroxyapatite is measured based on nitrogen desorption adsorption isotherms. Figure 3 shows the type of hydroxyapatite isotherm properties following type IV and H3 hysteresis loop type. The hydroxyapatite has a BET surface area of 138.20 m^2/g, while total pore volume and average pore diameter of hydroxyapatite were obtained 0.257 cm^3/g and 8.91 nm, respectively. The surface area of hydroxyapatite in this study had large than the commercial hydroxyapatite, which is 36.7 m^2/g [34].

3.2. Adsorption study

Interaction mechanism between Ni(II) with hydroxyapatite occurs in several ways. One of the possible mechanisms is through ion exchange. Calcium ions within hydroxyapatite were replaced by Ni(II) from solution. The adsorption process proceeds in 2 steps. The first step, Ni(II) rapidly adsorbed onto hydroxyapatite surface particularly at the POH groups a forms $Ca_{10-x}M_x(PO_4)_6(OH)_2$, the next step is substitution of Ca^{2+} by Ni^{2+}, according to reaction [21,39]:

$$Ca_{10}(PO_4)_6(OH)_2 + xM^{2+} \rightarrow Ca_{10-x}M_x(PO_4)_6(OH)_2 + xCa^{2+} \quad (2)$$

Another possible mechanism is through electrostatic attraction between hydroxyapatite and Ni (II). The solution pH influences the electrostatic attraction between hydroxyapatite and Ni(II). The pHpzc (Point zero charge) was determined using the pH drift method. The intersection between pH first and pH final is the pH_{PZC}. The pH_{PZC} of hydroxyapatite at 6.4 depicted in Figure 4. At solution pH < pH_{PZC}, the surface of hydroxyapatite is positively charged whereas, above the pH_{PZC}, the surface of hydroxyapatite became negatively charged.

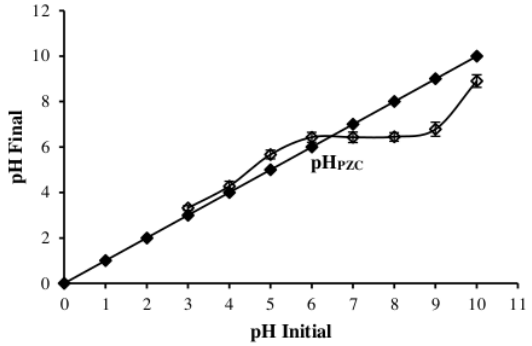

Figure 4. pH_{PZC} of hydroxyapatite

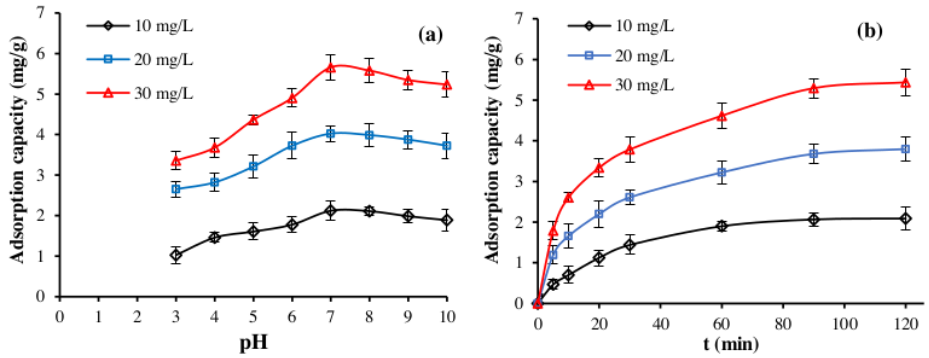

Figure 5. Sorption of Ni(II) by hydroxyapatite at (a) various pH and (b) contact time

Figure 5a confirmed that interaction is more effective above pH_{PZC}. Range of pH used in this work was 3-10. Adsorption capacity increased at pH 3 through pH 7. At low pH, Ni^{2+} and H^+ are positively charged, while hydroxyapatite is also positively charged, so there is an electrostatic repulsion. Increasing the pH of the solution so reducing H^+ in the solution [40]. If the pH of the solution > pH_{PZC}, H^+ become less available so that more Ni^{2+} is being adsorbed. Optimum pH for the adsorption process obtained in this work is 7 at all variation of Ni(II) concentrations. At this pH, hydroxyapatite is negatively charged, which attracts positively charge Ni^{2+} and raised its capacity. This is a common phenomenon in metal ions adsorption [41]. The optimum pH for Ni(II) adsorption reported by several authors at range 6-8 [4,10,41]. At pH 8, the adsorption capacity decreases. Ni(II) in the solution tends to precipitate to $Ni(OH)_2$ [10,42].

The effect of contact time against adsorption capacity of hydroxyapatite is illustrated in Figure 5b. The experiment was conducted at 3 different initial concentration of Ni(II) i.e. 10, 20 and 30 mg/L, the weight of hydroxyapatite 0.1 g, the contact time was varied from 0 to 120 minutes, stirring at 120 rpm and room temperature. These 2 steps of the adsorption process, initially Ni(II) is adsorbed rapidly until it reaches equilibrium i.e. the outer surface of hydroxyapatite becomes saturated. In this study, reached the equilibrium was obtained at 90 minutes. The second adsorption process occurred through the infiltration of Ni(II) into the inner surface of the adsorbent [21,40]. Adsorption duration effect at this stage is negligible because it happened indefinitely in time.

3.3. Adsorption kinetics

Mechanism of adsorption Ni(II) on hydroxyapatite was investigated through adsorption kinetic. Two models were presented i.e. pseudo-first-order and pseudo-second-order. The pseudo-first-order provides the most straightforward approach to describe solute adsorbed on the adsorbent; it is formulated as follows:

$$\log(q_e - q_t) = \log q_t - \frac{k_1}{2.303} t \quad (3)$$

q_e and q_t (mg/g) represent Ni(II) adsorbed at equilibrium and at t time respectively. k_1 is equilibrium constant for pseudo-first-order (1/min). The constant was obtained by plotting $\log(q_e - q_t)$ Versus t. Pseudo-second orde, on the other hand, presumed that adsorption occurs in chemisorption type [39]. The linear equation for this approach is formulated:

$$\frac{t}{q_e} = \frac{1}{k_2 q_e^2} + \frac{t}{q_e} \quad (4)$$

Plot of $\frac{t}{q_e}$ versus t the rate constant k_2 (g.mg^{-1}min^{-1}) can be determined. Figure 6 displays pseudo-first-order and pseudo-second-order plots, while Table 1 shows the kinetic parameter of Ni(II) with a concentration of Ni(II) is 10, 20 and 30 mg/L.

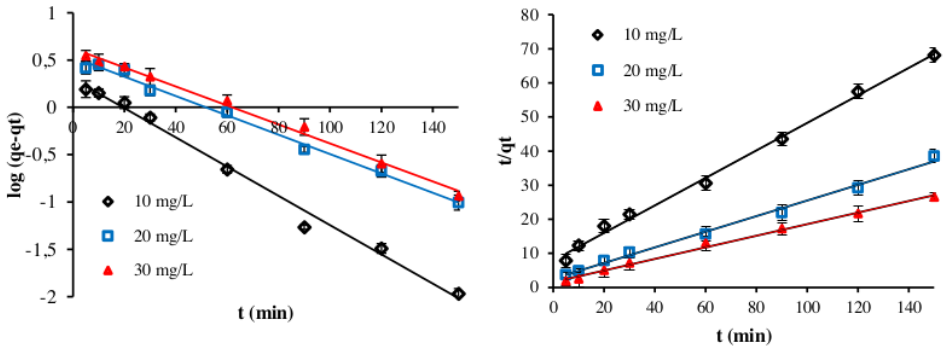

Figure 6. (a) Pseudo-first order dan (b) Pseudo-second order of Ni(II) sorption by hydroxyapatite

Table 1. The Kinetic parameters pseudo-first order and pseudo-second order.

Ni (II) (mg/L)	q_e (mg/g) Eksp.	Pseudo-first order			Pseudo-second order		
		q_e (mg/g) calculation	k_1 (1/min)	R^2	q_e (mg/g) calculation	k_2 (g/mg.min)	R^2
10	1.920	1.024	0.035	0.9924	2.481	0.0201	0.9956
20	3.811	1.026	0.025	0.9925	4.369	0.0200	0.9939
30	6.486	1.036	0.023	0.9933	5.886	0.0186	0.9946

Table 1 confirmed at increase Ni(II) concentration, the number of adsorbed ions also increase both experimentally and theoretically while the rate constants (k_1 dan k_2) tend to decrease. At a higher amount of Ni(II) adsorption, the surface of hydroxyapatite becomes saturated so that the rate will decrease. The coefficient of R^2 obtained for pseudo-second-order for all initial concentration of Ni(II) is higher than pseudo-first-order, indicated that adsorption of Ni(II) best fit to pseudo-second-order. Based on the result, it is likely that the adsorption process follows multistep chemisorption type [2]. A similar result has been reported in Ni(II) adsorption using activated carbon [6], moringa oleifera [10] and clay [39].

3.4. Adsorption thermodynamic

Thermodynamic of Ni (II) adsorption on hydroxyapatite was evaluated based on the value of Gibbs standard energy (ΔG^o), standard enthalpy (ΔH^o), and standard entropy (ΔS^o). The values of these three parameters can be determined by using the equation:

$$\Delta G^o = -RT \ln K \quad (5)$$

$$\Delta G^o = \Delta H^o - T\Delta S^o \quad (6)$$

$$\ln K = \frac{\Delta S^o}{R} - \frac{\Delta H^o}{RT} \quad (7)$$

K (L/g) is equilibrium constant, R is ideal gas constant ($8.314.10^{-3}$ KJ/mol.K), and T is temperature (K). Figure 7 illustrates the plot of ln K versus 1/T giving R^2 value of 0.9882. ΔH^o and ΔS^o were obtained from the slope and intercept; the overall calculation result is shown in Table 2. ΔG^o was found out negative at all temperature which concludes that adsorption occurs spontaneously. The value of ΔG^o decrease as temperature increase suggests the presence of electrostatic attraction results in an increase of adsorption capacity. Moreover, it reflects a favorable condition for the reaction at a higher temperature [10]. ΔH^o shows value for the endothermic process of adsorption whereas positive ΔS^o express the increase of hydroxyapatite affinity happened in random during adsorption of Ni(II).

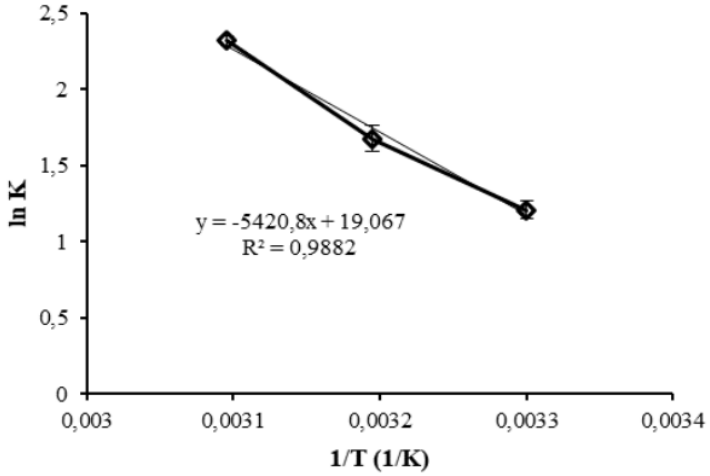

Figure 7. Plot of ln K Vs 1/T of Ni(II) sorption by hydroxyapatite

Table 2. Thermodynamic parameters of Ni(II) sorption by hydroxyapatite.

T (K)	$-\Delta G^o$ (KJ/mol)	ΔS^o (J/mol.K)	ΔH^o (KJ/mol)	R^2
303	3.048	0.158	45.068	0.9882
313	4.366			
323	6.230			

3.5. Adsorption Isotherm

The adsorption system design can be examined from adsorption isotherm [2]. Two adsorption isotherms were used in this work i.e. Langmuir and Freundlich. Langmuir isotherm assumed the adsorbent surface is homogeneous and each active site can absorb one molecule to form monolayer [21,43]. The Langmuir isotherm is as a follow:

$$\frac{C_e}{q_e} = \frac{C_e}{q_m} + \frac{1}{q_m} K_L \quad (8)$$

The concentration of Ni(II) at equilibrium denoted by C_e (mg/L), number of Ni(II) adsorbed per unit weight at equilibrium denoted by q_e (mg/g) and a maximum capacity of Ni(II) adsorbed express by q_m (mg/g). Constant related to adsorption energy is written as K_L (1/mg) which can be obtained from the plot $\frac{C_e}{q_e}$ versus C_e. Other than, Freundlich isotherm assumed heterogeneous system on hydroxyapatite. Mathematical expression for Freundlich isotherm is written as:

$$\ln q_e = \ln K_F + \frac{1}{n} \ln C_e \quad (9)$$

q_e (mg/g) represent the number of Ni(II) ion adsorbed per gram, K_F is Freundlich constant (mg/g) and the empirical constant is expressed as n, if $n < 1$, is unfavourable process, and $0 < n < 1$ is favourable process. Table 3 shows calculated adsorption isotherm parameters according to Langmuir and Freundlich models at room temperature. The Langmuir isotherm provides R^2 greater than Freundlich. So, the adsorption of Ni(II) to hydroxyapatite in accordance with the Langmuir model. The adsorption capacity of hydroxyapatite is obtained 5.359 mg/g. Freundlich parameter show $n > 1$, which implies a favorable adsorption process [44].

Table 3. Adsorption isotherm parameters of Ni(II) sorption onto hydroxyapatite.

Langmuir		**Freundlich**	
q_m **(mg/g)**	5.359	K_F (mg/g)	1.601
K_L **(L/mg)**	0.0273	n (g/L)	3.617
R^2	0.9916	R^2	0.9422

3.6. Morphology and elements of hydroxyapatite before and after Ni (II) sorption

Figure 8 depicted the hydroxyapatite morphology recorded by SEM. Hydroxyapatite has an irregular spherical shape, porous surface in an open pore mode. Agglomeration of hydroxyapatite appears as a consequence of nanosized material. Similar morphology has been reported by several authors who prepared hydroxyapatite with combustion method [29] and sol-gel methods [45] to obtain agglomerate and porous material. EDS hydroxyapatite data before and after adsorption is shown in Table 4. Hydroxyapatite consists of elements including O, Ca dan P, and after adsorption process, there is the addition of Ni. The elements of hydroxyapatite before adsorption had of O, Ca and P of 51.90, 33.04 dan 15.06%. The molar ratio (Ca/P) of hydroxyapatite is 1.70 approaching the theoretical 1.67. These results indicate that synthesized product has high purity. The composition of the elements after adsorption consisted of O, Ca, P, and Ni which each had values of 40.44, 35.49, 16.08, and 7.99%, respectively.

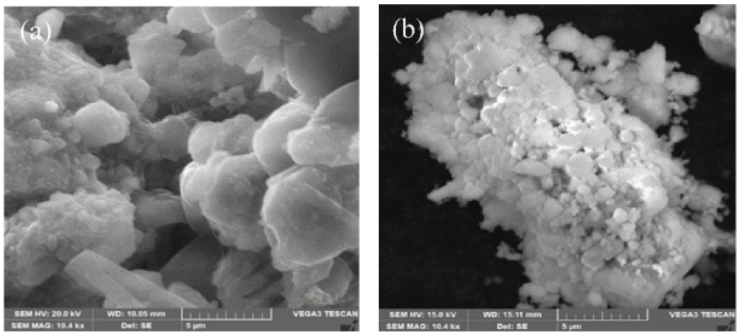

Figure 8. Morphology of hydroxyapatite (a) before and (b) after Ni(II) sorption

Table 4. Elements of hydroxyapatite before and after Ni(II) sorption.

Elements	**Hydroxyapatite**	
	Before adsorption (%)	After adsorption (%)
O	51.90	40.44
Ca	33.04	35.49
P	15.06	16.08
Ni	-	7.99

Table 5 shows the adsorption capacity of various adsorbents used in the reported removal of Ni(II) compared to this work. Many natural-based adsorbents have been developed recently. The main reason is economical and environmentally friendly. It seems that our results still have a low adsorption capacity compared to the others, but it shows high potential, especially in the elimination of Ni(II).

Table 5. Adsorption capacity comparison between various adsorbent for Ni(II) removal.

Adsorbent	**Adsorption capacity (mg/g)**	**References**
Clinoptilolite	5.08	46
Amine-functionalized modified rice straw	3.95	47
Granular activated carbon	1.49	48
Cucumis melo peel-activated carbon	5.43	49
Sewage sludge	11.52	50
Chitosan/diatomaceous earth composite	149.64	42
Spent coffee	57.14	51
Coffee husk	51.91	51
Hydroxyapatite	5.359	In this study

4. Conclusion

In this study, hydroxyapatite synthesized from snakehead fish bone by precipitation method has been successful. Hydroxyapatite was an effective biosorbent for removal Ni(II) from solution. Utilization of hydroxyapatite for Ni(II) adsorption was influenced by the pH of the solution, Ni(II) concentration and contact time. Finally, the adsorption of Ni(II) by hydroxyapatite follows pseudo-second-order kinetic approach and best described by Langmuir isotherm model with an adsorption capacity of 5.359 mg/g. Thermodynamic quantities concluded that adsorption occurs spontaneously and endothermically. Hydroxyapatite prepared from snakehead fish bone shows the potential for adsorption of Ni(II) from wastewater.

5. Acknowledgements

The author would like to thank for funding for Kementerian Riset Teknologi dan Pendidikan Tinggi Republik Indonesia *Hibah Penelitian Dasar Unggulan Perguruan Tinggi (PDUPT) grants* and Department of Chemistry, Sriwijaya University for research facilities.

References

1- S. L. Iconaru, M. M. Heino, R. Guegan, M. V. Predoi, A. M. Prodan, D. Predoi, Removal of zinc ions using hydroxyapatite and study of ultrasound behavior of aqueous media, Materials, **2018**, 11(1350), 1-16.
2- M. Mohammad, S. Maitra, N. Ahmad, A. Bustam, T. K. Sen, B. K. Dutta, Metal ion removal from aqueous solution using physic seed hull, J Hazard. Mater., **2010**, 179(1-3), 363-372.
3- P. K. Pandey, S. Choubey, Y. Verma, M. Pandey, S. S. K. Kamal, K. Chandrashekhar, Biosorptive removal of Ni(II) from wastewater and industrial effluent, Int. J. Environ. Res. Public Health, **2007**, 4(4), 332-339.
4- X. Zhang, X. Wang, Adsorption and desorption of nickel (II) ions from aqueous solution by a lignocellulose/montmorillonite nanocomposite, Plos One, **2015**, 3, 1-21.
5- M. A. Khan, M. Ngabura, T. S. Y. Choong, H. Masood, L. A. Chuah, Biosorption and desorption of nickel on oil cake: batch and column studies, Bioresour Technol., **2012**, 103(1), 35-43.
6- K. Kadirvelu, K. Thamaraiselvi, C. Namasivayam, Adsorption of nickel (II) from aqueous solution onto activated carbon prepared from coir pith, Sep Puri Technol., **2001**, 24(3), 497-505.
7- K. Allam, A. El Bouari, B. Belhorma, and L. Bih, Removal of Methylene Blue from Water Using Hydroxyapatite Submitted to Microwave Irradiation, J Water Resource Prot., **2016**, 8(3), 358-371.
8- G. Ciobanu, S. Barna, M. Harja, Kinetic and equilibrium studies on adsorption of Reactive Blue 19 dye from aqueous solutions by nanohydroxyapatite adsorbent, Arch. Environ. Prot., **2016**, 42(2), 3-11.
9- N. A. M. Barakat, M. S. Khil, A. M. Omran, F. A. Sheikh, H. Y. Kim, Extraction of pure natural hydroxyapatite from the bovine bones biowaste by three different methods, J. Mater. Process. Technol., **2009**, 209(7), 3408-3415.
10- H. K. Reddy, D. K.V. Ramana, K. Seshaiah, A. V. R. Reddy, Biosorption of Ni(II) from aqueous phase by Moringa Oleifera bark, a low-cost biosorbent, Desalination, **2017**, 268 (1-3),150-157.
11- N. Singh, and R. Gadi, Removal of Ni(II) and Cu(II) from their solutions and wastewater by nonliving biomass of *Pseudomonas Oleovorans*, Hydrol Current Res., **2012**, 3(1), 1-4.
12- M. Boutinguiza, J. Pou, R. Comesana, F. Lusquifios, A. de Carlos, B. Leon, Biological hydroxyapatite obtained from fish bone, Mater Sci Eng C, **2012**, 32(3), 478-486.
13- H. Zhou, J. Lee, Nanoscale hydroxyapatite particles for bone tissue engineering, Acta Biomater, **2011**, 7(7), 2769-2781.
14- S. M. Mousa, N. S. Ammar, H. A. Ibrahim, Removal of lead ions using hydroxyapatite nano-material prepared from phosphogypsum waste, J Saudi Chem Soc., **2016**, 20(3), 357-365.
15- S. C. Wu, H. C. Hsu, S. K. Shu, Y. C. Chang, Wen. F. Ho, Synthesis of hydroxyapatite from eggshell powders through ball milling and heat treatment, J Asian Ceram Soc., **2016**, 4(1), 85-90.
16- P. Joshi, S. Manocha, Kinetic and thermodynamic study of the adsorption of copper ions on hydroxyapatite nanoparticles, Mater Today, **2017**, 4(9), 10455-10459.
17- S. George, D. Mehta, V. K. Saharan, Application of hydroxyapatite and its modified forms as adsorbents for water defluoridation: an insight into process synthesis, Rev Chem Eng., **2018**, 1-32.
18- Y. Nishiyama, T. Hanafusa, J. Yamashita, Y. Yamamoto, T. Ono, Adsorption and removal of strontium in aqueous solution by synthetic hydroxyapatite, J Radioanal Nucl Chem., **2016**, 307(2), 1279-1285.
19- M. Harja, G. Ciobanu, Removal of oxytetracycline from aqueous solutions by hydroxyapatite as a low-cost adsorbent, in International Conference on Advances in Energy Systems and Environmental Engineering (ASEE17), Poland, July 2-5, **2017**, 1-8.
20- Y. Song, J. Gao, Y. Zhang, S. Song, Preparation and characterization of nano-hydroxyapatite and its competitive adsorption kinetics of copper and lead ions in water, Nanomater Nanotechno., **2016**, 6(1-8), 1-8.
21- S. M. H. Dabiri, A. A. Rezaie, M. Moghimi,

H. Rezaie, Extraction of Hydroxyapatite from Fish Bones and Its Application in Nickel Adsorption, BioNanoScience, **2018**, 8(3), 823-834.

22- M. Mourabet, A. El Rhilassi, H. El. Boujaady, M. B. Ziatni, R. El. Hamri, A. T. Tai, Removal of fluoride from aqueous solution by adsorption on hydroxyapatite (HAp) using response surface methodology, J Saudi Chem Soc, **2015**, 19(6), 603-615.

23- B. R. Sunil, M. Jagannatham, Producing hydroxyapatite from fish bones by heat treatment, Mater Lett., **2016**, 185, 411-414.

24- S. Rujitanapanicha, P. Kumpapanb, P. Wanjanoic, Synthesis of Hydroxyapatite from Oyster Shell via Precipitation, Energy Procedia, **2014**, 56, 112-117.

25- M. F. Alif, W. Aprillia, S. Arief, Peat water purification by hydroxyapatite (HAp) synthesized from waste pensi (*Corbicula moltkiana*) shells, in International Conference on Chemistry and Material Science (IC2MS), Malang Indonesia, 4-5 November **2017**, pp. 1-6.

26- R. N. Granito, A. C. M. Renno, H. Yamamura, M. C. de Almeida, P. L. M. Ruiz, D. A. Ribeiro, "Hydroxyapatite from fish for bone tissue engineering: A Promising Approach, Int. J. Mol. Cell. Med. Spring, **2018**, 7(2), 80-90.

27- K. Allam, A. El Bouari, B. Belhorma, L. Bih, Removal of methylene blue from water using hydroxyapatite submitted to microwave irradiation, J Water Resource Prot., **2016**, 8, 358-371.

28- B. A. E. Ben-Arfa, I. M. M. Salvado, J. M. F. Ferreira, Nouvel route for the rapid sol-gel synthesis of hydroxyapatite, avoiding ageing and using fast drying with a 50-fold to 200-fold reducting in process time, Mater Sci Eng C Mater Biol Appl., **2017**, 70(1), 796-804.

29- M. Canillas, R. Rivero, R. G. Carrodeguas, F. Barba, M. A. Rodriguez, Processing of hydroxyapatite obtained by combustion synthesis, Bol Soc Esp Ceram V, **2017**, 56(5), 237-242.

30- W. Kim, F. Saito, Sonochemical synthesis of hydroxyapatite from H_3PO_4 solution with $Ca(OH)_2$, Ultrason Sonochem., **2001**, 8(2), 85-88.

31- I. Mobasherpour, M. S. Heshajin, A. Kazemzadeh, M. Zakeri, Synthesis of nanocrystalline hydroxyapatite by using precipitation method, J Alloys Compd., **2007**, 430(1-2), 330-333.

32- M. Okada, T. Matsumoto, Synthesis and modification of apatite nanoparticles for use in dental and medical applications, Jpn Den Sci Rev., **2015**, 51(4), 85-95.

33- W. Wei, L. Yang, W. Zhong, J. Cui, Z. Wei, Poorly crystalline hydroxyapatite: A novel adsorbent for enhanced fulvic acid removal from aqueous solution, **2015**, Appl Surf Sci., 332, 328-339.

34- A. R. Ibrahim, Y. Zhou, X. Li, L. Chen, Y. Hong, Y. Su, H. Wang, J. Li, Synthesis of rod-like hydroxyapatite with high surface area and pore volume from eggshells for effective adsorption of aqueous Pb(II), Mater Res Bull., **2015**, 62, 132-141.

35- M. S. Shojai, M. T. Khorasani, E. D. Khoshdargi, A. Jamshidi, Synthesis methods for nano size hydroxyapatite in diverse structures, Acta Mater., **2013**, 9(8), 7591-7621.

36- A. Pal, S. Paul, A. R. Choudhury, V. K. Balla, M. Das, and A. Sinha, Synthesis of hydroxyapatite from Lates calcarifer fish bone for biomedical applications, Mater Lett., **2017**, 203, 89-92.

37- P. Wang, C. Li, H. Gong, X. Jiang, H. Wang, K. Li, Effect of synthesis conditions on the morphology of hydroxyapatite nanoparticles produced by a wet chemical process, Powder Technol., **2010**, 2013(2), 315-321.

38- P. Kamalanathan, S. Ramesh, L. T. Banga, A. Niakan, C.Y. Tan, J. Purbolaksono, H. Chandran, W. D. Teng, Synthesis and sintering of hydroxyapatite derived from eggshells as a calcium precursor, Ceram Int., **2014**, 40(10), 16349-16359.

39- S. S. Gupta, K. G. Bhattacharya, Adsorption of Ni(II) on clays, J Colloid Interface Sci., **2016**, 295(1), 21-32.

40- S. S. Salih, T. K. Ghosh, Preparation and characterization of bioadsorbent beads for chromium and zink ion adsorption, Cogent Environ Sci., **2017**, 3, 1-14.

41- I. Mobasherpour, E. Salahi, M. Pazouki, Comparative of the removal of Pb^{2+}, Cd^{2+} and Ni^{2+} by nano crystallite hydroxyapatite from aqueous solutions: Adsorption isotherm study, Arab J Chem., **2012**, 5(4), 439-446.

42- S. S. Salih, T. K. Ghosh, Highly efficient competitive removal of Pb(II) and Ni(II) by chitosan/diatomaceous earth composite, J Environ Chem Eng., **2018**, 6(1), 435-443.

43- S. S. Salih, T.K. Ghosh, Preparation and characterization of chitosan-coated diatomaceous earth for hexavalent chromium removal, Environ. Process, **2018**, 5, 23-39.

44- A. I. Adeogun, E. A. Ofudje, M. A. Idowu, S. O. Kareem, S. Vahidhabanu, B. R. Babu, Biowaste-derived hydroxyapatite for effective removal of reactive yellow 4 dye: equilibrium, kinetic, and thermodynamic studies, ACS Omega, **2018**, 3(2), 1991-2000.

45- I. Kim, P. N. Kumta, Sol-gel synthesis and characterization of nanostructured hydroxyapatite powder, Mater Sci Eng B., **2004**, 111(2-3), 232–236.

46- O. Oter, H. Akcay, Use of natural clinoptilolite to improve water quality: sorption and selectivity studies of lead (II), copper (II), zinc(II), and nickel (II), Water Environ Res., **2007**, 79(3), 329-335.

47- W. Yunhai, F. Yiang, Z. Meili, M. Zhu, Y. Shengxin, A. Aynigar, F. Peng, Functionalized agricultural biomass as a low-cost adsorbent: Utilization of rice straw incorporated with amine groups for the adsorption of Cr(VI) and Ni(II) from single and binary systems, Biochem Eng J., **2016**; 105, 27-35.
48- K. Periasamy, C. Namasivayam, Removal of nickel(II) from aqueous solution and nickel plating industry using agricultural waste: peanut hulls, Waste Manage., **1995**, 15(1), 63-68.
49- M. Manjuladevi, R. Anitha R. and S. Manonmani, Kinetic study on adsorption of Cr(VI), Ni(II), Cd(II) and Pb(II) ions from aqueous solutions using activated carbon prepared from *Cucumis melo* peel, Appl Water Sci., **2018,** 8(36), 1-8.
50- O. Khelifi, M. Nacef, A. M. Affoune, Nickel (II) Adsorption from Aqueous Solutions by Physico-Chemically Modified Sewage Sludge, Iran J Chem Eng., **2018**; **37**: 73-87.
51- M. H. Rodiguez, J. Yperman, R. Carleer, J. Maggen, D. Dadi, G. Gryglewicz, B. V. der Bruggen, J. F. Hernandez, A. O. Calvis, Adsorption of Ni(II) on spent coffee and coffee husk based activated carbon, J Environ Chem Eng, **2018**, 6(1), 1161-1170.

Medjem 2019

ORIGINALITY REPORT

4%	4%	2%	1%
SIMILARITY INDEX	INTERNET SOURCES	PUBLICATIONS	STUDENT PAPERS

MATCH ALL SOURCES (ONLY SELECTED SOURCE PRINTED)

4%

★ idoc.pub

Internet Source

Exclude quotes	On	Exclude matches	< 1%
Exclude bibliography	On		